Nuclear Instruments and Methods in Physics Research B 342 (2015) 166–169

Contents lists available at ScienceDirect

Nuclear Instruments and Methods in Physics Research B

journal homepage: www.elsevier.com/locate/nimb

Target depth dependence of damage rate in metals by 150 MeV proton irradiation

T. Yoshiie *, Y. Ishi, Y. Kuriyama, Y. Mori, K. Sato, T. Uesugi, Q. Xu

Research Reactor Institute, Kyoto University, Kumatori, Sennan, Osaka 590-0494, Japan

ARTICLE INFO

Article history:
Received 30 July 2014
Received in revised form 29 September 2014
Accepted 30 September 2014

Keywords:
Proton irradiation
Target thickness dependence of damage rate
Ni
Electrical resistance measurement
Positron annihilation lifetime measurement

ABSTRACT

A series of irradiation experiments with 150 MeV protons was performed. The relationship between target depth (or shield thickness) and displacement damage during proton irradiation was obtained by in situ electrical resistance measurements at 20 K. Positron annihilation lifetime measurements were also performed at room temperature after irradiation, as a function of the target thickness. The displacement damage was found to be high close to the beam incident surface area, and decreased with increasing target depth. The experimental results were compared with damage production calculated with an advanced Monte Carlo particle transport code system (PHITS).

1. Introduction

The structural damage by high-energy particles is usually expressed as an average displacement per atom (DPA). In order to obtain the DPA, it is necessary to calculate the energy deposited by the irradiation in a material (also called primary recoil energy). Irradiated low-energy particles, such as ions, electrons, and neutrons, mainly interact with atoms in the matter via elastic scattering, and the damage can be accurately modeled [1,2]. The damage caused by high-energy particles, instead, is more difficult to calculate, since they interact with matters through nuclear reactions. In this particular case, the DPA is usually calculated with advanced Monte Carlo particle transport codes, such as LAHET [3], MCNP [4], FLUKA [5], MARS [6] and PHITS [7]. These codes can model nuclear reactions and the creation of secondary particles, and they are widely used in the field of radiation protection and for the prediction of materials lifetime at high-energy ion beam facilities. These codes can make use of available nuclear data and they utilize the most recent nuclear reaction models. The accuracy of the predictions, however, still needs experimental verifications. The measurement of nuclear products by detecting the radioactivity of materials after irradiation, for example, can be compared with the results of the codes. Unfortunately, it is not possible to demonstrate the accuracy of quantities that are impossible to measure experimentally, such as the energy deposited in a material by irradiation. As a famous precedent, Kiritani et al. estimated the deposited energy in subcascades created by fusion neutron irradiation experimentally, however, using the primary recoil energy spectra calculated from a code [8].

High-energy particle irradiation simulations predict that the displacement rate due to damage is almost independent of the target depth for ranges lower than the Bragg peak (also called ion stopping range). At the peak, the displacement damage rate is the highest and decreases drastically after that range [9]. Recently, we obtained an experimental result that differs from these predictions. In this paper, we describe experimental measurements of the displacement damage rate as a function of the target depth (shield thickness), performed with two independent methods: the electrical resistance at low temperatures, and the positron annihilation lifetimes at room temperature. We also report a comparison of the experimental results with the predictions calculated with PHITS code.

2. Experimental procedure

2.1. Proton accelerator

The specimen was irradiated with a 150 MeV proton beam, using the newly developed Fixed-Field Alternating-Gradient (FFAG) accelerator at the Research Reactor Institute, Kyoto University, Japan. Nonlinear magnetic fields can be effectively utilized using accelerators based on the FFAG principle, which is not possible with ordinary accelerators [10]. For an injector, an 11 MeV linear accelerator (H^- ions) was connected to the FFAG ring.

* Corresponding author.

http://dx.doi.org/10.1016/j.nimb.2014.09.037
0168-583X/

2.2. Electrical resistance measurements

The electrical resistance of a Ni wire (99.99%, 0.1 mm in diameter) was measured at 20 K during proton irradiation, using the setup shown in Fig. 1. The irradiation was performed in a vacuum chamber (1×10^{-5} Pa), where a Ni wire was wounded on a sapphire plate of 1.0 mm in thickness. The plate was sandwiched with two Al plates, covered with an insulating 12.5-μm-thick Kapton® polyimide tape. The Al plates were bolted to a Cu heat-conduction column of a refrigerator (RDK-205E, Sumitomo Heavy Industries, Ltd.) having a cooling capacity of 0.5 W. The Cu column was covered with an Al thermal shield, composed of a pipe of 50 mm in diameter and 3 mm in thickness. Two Al beam windows of 3 mm in thickness were located at the end of beam duct of the FFAG accelerator and the beam entrance of the irradiation chamber, separated by a space of 30 mm. The Cu plate was inserted between the windows. The change of Cu thickness corresponded to the target depth change. The distance between the Al beam window protecting the irradiation chamber and the Ni wire was about 470 mm. The Cu plate was placed in contact with Al beam window. The temperature was measured using a Au–Fe type thermocouple. The electrical resistance was measured with the four-probe DC technique. In order to get rid of unwanted thermoelectric effects, the current direction was changed every 0.1 s. The voltage was measured using a National Instruments Compact DAQ NI 9219 analogue/digital converter, remotely connected to LabVIEW. The data were collected every 5 s, at proton beam intensity of 1.8×10^8 p/cm^2/s.

2.3. Positron annihilation lifetime measurements

Positron annihilation spectroscopy can be used to detect small vacant sites, which are below the resolution limit of transmission electron microscopy. The positron is the only probe that can sensitively detect vacancy-type defects in most materials. High-energy positrons generated from the β+ decay of a radioactive source (e.g., Na-22) are injected into materials. These positrons are rapidly thermalized and annihilated with electrons. If there are open spaces in the lattice, such as vacancies, where positively charged nuclei are absent, the positrons are briefly trapped there, resulting in a longer lifetime. The increased lifetime depends on the type and size of the defects and therefore conveys important information regarding vacancy-type defects and edge dislocations.

The positron annihilation lifetime of the studied specimens was measured at room temperature using a conventional fast–fast spectrometer with a time resolution of 190 ps (full width at half maximum), until a total integrated count of 1×10^6 was reached. The positron lifetime spectra were analyzed using the PALSfit program [11] and, when possible, the lifetimes were decomposed into two components: τ_1 and τ_2. Otherwise, only a mean lifetime τ_m was obtained. The longer lifetime, τ_2, and the corresponding intensity, I_2, indicate the size and the concentration of defect clusters, respectively [12]. One set of specimens was composed of six discs made of different metals: two Ni (99.99%) discs, two Au (99.999%) discs, and two made of Cu (99.999%). Each disc measured 3 mm in diameter and 0.1 mm in thickness. Six sets of specimens were stacked inside a Pb cavity and irradiated as shown in Fig. 2 to study the target depth dependence of displacement damage. The positron annihilation lifetime was measured with a Na-22 positron source sandwiched between two discs located at the same position, after the proton irradiation.

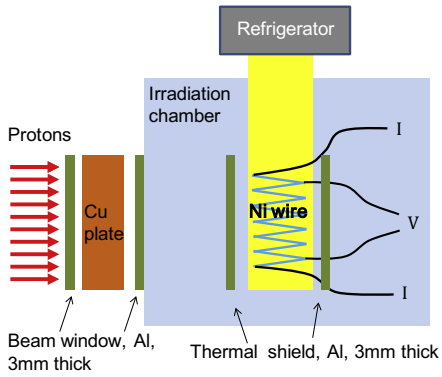

Fig. 1. Schematic illustration of the setup used for the electrical resistance measurements. The electrical resistance of the Ni wire (0.1 mm in diameter) in the irradiation chamber was measured at 20 K during proton irradiation. A Cu plate was inserted between the two beam windows.

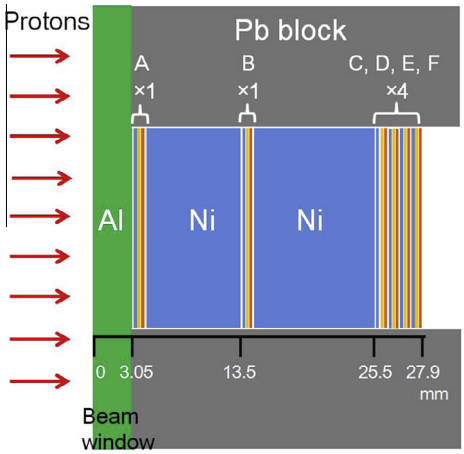

Fig. 2. Schematic illustration of six specimen positions (A–F) in a cavity of 3.2 mm in diameter, inside a Pb block of $40 \times 40 \times 38$ mm^3 for 150 MeV proton irradiation at room temperature. At each position, six specimens (two Ni, two Au, and two Cu discs) of 0.1 mm thickness and 3 mm diameter were inserted.

3. Results

3.1. Electrical resistance measurements

Upon irradiation damage, defects are formed in the exposed material; in the case of a metallic specimen, its electrical resistance increases. The electrical resistance changes during a continuous irradiation were measured for 5 min as a function of the Cu plate thickness, at a temperature of 20 K. By increasing the thickness of the Cu plate, we observed a reduction of the increase rate of the electrical resistance, as shown Table 1. It should be noticed that even 0 mm Cu case, the Ni wire was irradiated with the proton beam that went through three Al plates of 9 mm in total (two Al beam windows of 3 mm in thickness and one Al thermal shield of 3 mm in thickness) as shown in Fig. 1. The highest increase rate, in particular, was observed when the Cu plate was missing. Since the recovery of point defects in Ni only occurs at temperatures above 30 K [13], no annealing effects were expected during the measurements.

3.2. Positron annihilation lifetime measurements

Positron annihilation lifetimes were measured after an irradiation to a flux of 2.5×10^{14} protons/cm^2, at room temperature. The positron annihilation lifetimes of Ni, Au and Cu at the various specimen positions (A–F) are reported in Table 2. It should be noticed that before the specimens at "A", there existed the Al beam win-

Table 1
Resistance increase rate of the Ni wire for the corresponding Cu plate thickness, irradiated with a 150 MeV proton beam at 20 K. Below: displacement cross-sections calculated by the PHITS code [15].

Thickness of the Cu plate (mm)	0	10	20	22	23	25
Resistance increase rate (10^{-8} Ω/s)	6.4	3.9	3.4	3.2	1.9	1.7
Displacement cross-section (dpa 10^{-21} cm^2/p)	2.21	2.15	2.35	2.53	3.66	2×10^{-3}

Table 2
Positron annihilation lifetimes and the intensity of long lifetimes of Ni, Au, and Cu, irradiated with a 150 MeV proton beam at different specimen positions (as shown in Fig. 2). '–' indicates that the two component analysis was impossible.

	Mean lifetime	Short lifetime	Long lifetime	Intensity of long lifetime I_2 (%)
	τ_m (ps)	τ_1 (ps)	τ_2 (ps)	
Ni position				
A	111 ± 1	104 ± 1	256 ± 24	3 ± 1
B	110 ± 1	101 ± 1	192 ± 22	7 ± 3
C	107 ± 1	–	–	–
D	108 ± 1	–	–	–
E	108 ± 1	–	–	–
F	107 ± 1	–	–	–
Au position				
A	131 ± 1	105 ± 1	188 ± 9	28 ± 5
B	128 ± 1	115 ± 1	209 ± 18	11 ± 4
C	124 ± 1	–	–	–
D	121 ± 1	–	–	–
E	119 ± 1	–	–	–
F	120 ± 1	–	–	–
Cu position				
A	116 ± 1	110 ± 1	265 ± 49	2 ± 1
B	116 ± 1	111 ± 1	380 ± 49	1 ± 1
C	113 ± 1	–	–	–
D	111 ± 1	–	–	–
E	111 ± 1	–	–	–
F	111 ± 1	–	–	–

dow of 3.05 mm in thickness (Fig. 2). The specimen set at "F" was irradiated with the proton beam that went through Al of 3.05 mm, Ni rods of 21.25 mm and 5 specimen sets (the total thickness of 3 mm, including Au of 1 mm). For all the probed positions, the lifetimes were higher than those of the unirradiated specimens (Ni: 106 ps, Au: 115 ps, Cu: 108 ps), indicating the formation of irradiation defects. In particular, the lifetimes measured at A and B (closer to the proton beam incident surface) were the highest for all the probed specimens. Since the lifetimes of single vacancies in metals are about 180 ps [14], we expect that vacancies and small vacancy clusters were formed in all the three metals, when exposed at A and B.

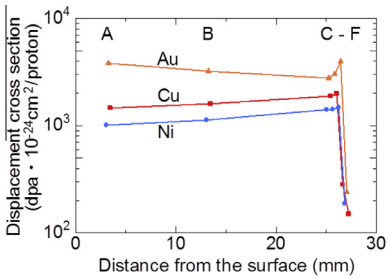

Fig. 3. Displacement cross-sections calculated by the PHITS code [15]. The distance from the surface is calculated at the positions depicted in Fig. 2.

4. Estimation of damages

The displacement damage produced by the proton irradiation was calculated by using the PHITS code [15]. The simulations were performed to reproduce the experimental measurements. The NRT formalism [16] was used to estimate the displacement cross-sections. The calculated damage cross-section (expressed in dpa·cm^2) of the Ni wire in the system depicted in Fig. 1 is shown in Table 1, as a function of Cu plate thickness inserted in two Al windows. The displacement threshold energy was set to 40 eV. The simulations predict almost the same damage up to a Cu thickness of 20 mm. Above that threshold, the cross-section increases up to a thickness of 23 mm and then decreases remarkably. The observed increment is caused by the Coulomb scattering near the Bragg beak. After the decrease, the displacement cross-section was less than 10^{-3} of the maximum value, and does not change for thicknesses above 25 mm. Because damages in this area were formed by neutrons generated with nuclear reactions and had little thickness dependence.

The displacement cross-sections of Ni, Au, and Cu, for the case of the positron annihilation lifetime measurements in the system depicted in Fig. 2, are shown in Fig. 3. Displacement threshold energies of 40 eV, 30 eV, and 30 eV were used for Ni, Au, and Cu, respectively (15). The target depth dependence does not change significantly up to a thickness of 25 mm. These results were supported by calculations reported in the literature [9].

5. Discussion

The two independent experiments performed indicated that the displacement damage was the highest at the beam incident region, but its result could not be reproduced by the PHITS code. We propose two hypotheses to explain the discrepancy: the limitation of simulation code, and the geometrical factors. The calculation code,

indeed, only considers the formation of secondary particles, but does not include the effects of particles formed by higher reactions. Similarly, the code does not include secondary effects due to the particular geometry of the experiments. In particular, the setup used for measuring the electrical resistance presents spaces between the Cu plate and the beam windows, between the beam window and the Al thermal shield, and between the thermal shield and the Ni wire. In the real experiment, the resistance increase rate did not change much between the 10 mm and the 25 mm Cu plate that was inserted into Al plates of 9 mm in total thickness, while the calculated displacement cross-section changed by less than 0.001 as shown in Table 1. The high resistance increase rate may be caused by high-energy particles spattered in the irradiation chamber. In the case of the positron annihilation lifetime measurements, the specimens were stacked to each other, so the surface spattering may also contribute to the damage production: a process that is not included in the code. For both the electrical resistance and the positron annihilation lifetime measurements, the increase of displacement damages near the Bragg peaks was not detected, because the recorded peak is too sharp (full width at half maximum: 0.1 mm) to measure the damages of the peak position.

6. Concluding remark

In this paper, we presented two irradiation experiments aimed to study the dependence of the target depth on the damage production. The experimental results differed from the predicted calculations by using the PHITS code. The reason of this discrepancy is still not entirely clear, but it can be related to geometrical factors not included in the simulations. We believe that the codes should include such information, in order to help the design of nuclear systems.

Acknowledgements

This study was a result of "Clarification of material behaviors in accelerator driven systems by an FFAG accelerator", carried out under the Strategic Promotion Program for Basic Nuclear Research by the Ministry of Education, Culture, Sports, Science and Technology of Japan.

References

[1] J.P. Biersack, L.G. Haggmark, Nucl. Instr. Meth. 174 (1980) 257.
[2] L.R. Greenwood, R.K. Smither, "SPECTER: Neutron Damage Calculations For Materials Irradiations", ANL/FPP/TM-197 (January 1985).
[3] R.E. Prael, H. Lichtenstein, "User Guide to LCS: The LAHET Code System", LA-UR-89-3014, Los Alamos National Laboratory, 1989.
[4] L.S. Water (Ed.), MCNPX User's Manual version 2.4.0, LA-CP-02-408, Pergamon Press, New Jersey, 2002.
[5] A. Fasso, A. Ferrari, J. Ranft, P.R. Sala, FLUKA: a multi-particle transport code CERN-2005-10, 2005, INFN/TC_05/11, SLAC-R-773.
[6] N.V. Mokhov, S.I. Striganov, MARS15 Overview, in: Proceeding of Hadronic Shower Simulation Workshop, Fermilab, September 2006, AIP Conf. Proc. 896, 2007, p. 50–60. <http://www-ap.fnal.gov/MARS/>.
[7] T. Sato, K. Niita, N. Matsuda, S. Hashimoto, Y. Iwamoto, S. Noda, T. Ogawa, H. Iwase, H. Nakashima, T. Fukahori, K. Okumura, T. Kai, S. Chiba, T. Furuta, L. Sihver, J. Nucl. Sci. Technol. 50 (2013) 913.
[8] M. Kiritani, T. Yoshiie, S. Kojima, Y. Satoh, Radiat. Eff. Defects Solids 113 (1990) 75.
[9] Y. Iwamoto, K. Niita, T. Sawai, R.M. Ronningen, T. Baumann, Nucl. Instr. Meth. Phys. Res. B 303 (2013) 120.
[10] Y. Mori, Proc. IPAC 2012, New Orleans, 2012, p. 10541058. <http://appora.fnal.gov/pls/ipac12/TOC.htm>.
[11] P. Kirkegaard, J.V. Olsen, M. Eldrup, N.J. Pedersen, Riso DTU, February 2009, ISBN 978-87-550-3691-8, p. 44, <http://palsfit.dk/>.
[12] W. Brandt, A. Dupasquier, Positron Solid-State Physics, North-Holland, Amsterdam, 1983.
[13] H. Knöll, U. Dedek, W. Schilling, J. Phys. F Metal Phys. 4 (1974) 1095.
[14] H. Ohkubo, Z. Tang, Y. Nagai, M. Hasegawa, T. Tawawa, M. Kiritani, Mater. Sci. Eng. A 350 (2003) 95.
[15] Y. Iwamoto, H. Iwamoto, M. Harada, K. Niita, J. Nucl. Sci. Technol. 51 (2014) 98.
[16] M.J. Norgett, M.T. Robinson, I.M. Torrens, Nucl. Eng. Des. 33 (1975) 50.